Nanograin VO_2 in the metal phase : a plasmonic system with falling dc resistivity as temperature rises

A Gentle, A I Maaroof and G B Smith
Institute of Nanoscale Technology, University of Technology, Sydney;
PO Box 123 Broadway NSW 2007 Australia

E-mail: amaaroof@uts.edu.au

Abstract Thin films of vanadium dioxide with grain sizes smaller than 60 nm have a metallic phase with excellent plasmonic response, but their dc resistivity falls as temperature rises to values well above the metal-insulator transition. At the transition optical switching is complete, but the switch in dc resistance is incomplete. In the metallic phase nanograin and large grain samples have similar values of both plasma frequency and relaxation rate. However plasmonic response in nanograins is stronger due to the absence of a low energy interband transition found in large grain films. Conductivity rises with a thermal activation energy of 108 meV, which is well below that in the semiconductor phase. Possible mechanisms for "non-metal-like" dc behaviour in this plasmonic system are briefly discussed. They include fluctuations which are coherent in nanograins but incoherent for larger grains. Nanoscale systems seem preferable for optical switching applications and large grain structures for dc switching work.

Keywords: vanadium dioxide; thin film; thermochromic; optical properties; resistance; plasmonics; nanostructure

PACS: 71.30. h; 73.61.-r; 78.20.-e

1. Introduction

There are many known metal insulator transitions (MIT) [1] but the one that so far has had most technological potential is that in vanadium dioxide. Therefore it has been extensively studied experimentally in a variety of bulk and thin film structures, and more recently as nanoparticles [2]. Despite this, many features such as a very fast relaxation rate in the metal phase [3,4], are yet to be satisfactorily explained, while new behaviours continue to emerge in various nanostructures or with process variations and doping. From recent studies on nanoparticles [2,5] and

nanostructured thin films [6, 7] it is apparent that key properties can be sensitive to variations in grain size, as well as particle shape and size. In the case of thin films a change in thickness is also known to effect basic parameters.

This study of nanostructured thin layers is focussed on the high temperature rutile phase, which is metallic. The observations of most interest are the dc resistivity, and the Drude response at near-infra red (NIR) frequencies. In these films the NIR behaviour is clearly metallic in character, but the dc response to temperatures well above the transition temperature is not metal-like. In normal metals dc resistivity and Drude response are closely linked since they require near matching values of carrier density, effective mass and carrier relaxation times. However in metallic VO_2 the values of these parameters as found in both types of experiment are less closely linked, and the difference between the optical and dc predictions is quite sensitive to structure. In other words if we estimate dc resistivity from Drude parameters, the variance with observed resistivity covers an extensive range as sample structure varies. In VO_2 the Drude parameters tend to underestimate the metal's dc resistivity ρ by at least an order of magnitude [4,8,9]. However in many thin films, including those we present in this study, this underestimate of ρ via Drude parameters can be as high as three orders of magnitude. Associated with these larger differences is a smaller sharp drop in ρ as T is raised through the transition at $T = T_c$. Explanations of known transport anomalies in the VO_2 metal phase have included strong frequency dependent relaxation rates or effective masses [9] but such phenomenological treatments are sample dependent and assume constant carrier density. To gain further insights we have studied the resistivity and optical permittivity in thin 'metallic' films with nano-sized grains to establish the strength of their plasmonic behaviour. Despite their dc behaviour, these nanostructures are more strongly plasmonic in the NIR than large grain films and bulk crystals. This interesting fact means that nanostructures and nanoparticles may be more useful for optical work than large grained, dense structures. It also means that theoretical models of optical response in VO_2 nanostructures should not use data obtained on bulk crystals or large grain films. This is not for the usual reason of enhanced relaxation rates in the small scale structures, since in VO_2 that is not an influence as we shall demonstrate; rather it seems to be intrinsic to the overall electronic structure when there is some nanoscale confinement.

It is the strength of the plasmonic response which is crucial to many of the proposed applications of VO_2. In films it determines the magnitude of NIR reflectance, and the rate at which spectral reflectance $R(\lambda)$ rises as wavelength λ increases above 900 nm. In nanoparticles it influences the strength of surface plasmon resonant absorption. The strength of plasmonic response is governed by the real part of permittivity $Rl(\varepsilon)$ of the metallic phase, which must be negative below a given frequency. In strongly plasmonic systems the magnitude of $Rl(\varepsilon)$ can become quite large. A fast rate of decrease of $Rl(\varepsilon)$ with increase in wavelength is also a good indicator of a strong plasmonic system. In our samples it becomes negative near 900 nm. Reported plasmonic behaviour in the metal phase, including some bulk crystal data and thin film data [4], covers a wide range from complete absence to the strong values of the samples in this report. One example [10] has a narrow window of weak plasmonic response from 1.2 to 4.8 μm, above which it is

again non–plasmonic. While a high plasma frequency is needed, two factors dampen plasmonic response in VO_2 (i) the anomalously high conduction electron relaxation frequency in the NIR which is of order 0.7 eV to 1 eV (ii) the existence in many samples of a low energy transition around 0.7 to 0.8 eV, with significant spectral weight [4,10]. From data on oriented bulk crystals this low energy transition seems to occur for fields normal to the c-axis but not parallel to it. It is also consistent with recent near-Fermi level band structures for rutile phase crystal field orbitals in this direction [11]. Such transitions will be shown to be absent in optical spectra on our nano-grain samples for normal incidence. This absence, coupled with their excellent plasma frequency leads to these thin VO_2 films being among the strongest from a plasmonic perspective, of any reported to date.

2. Experimental details

2.1 Film deposition

Vanadium metal thin films were first prepared by DC magnetron sputtering onto optically polished super-white glass (76×26×1 mm^3) substrates after ultrasonically cleaning with detergent solution for 20 minutes followed by rinsing with distilled water and drying with high purity nitrogen gas. The vanadium sputtering targets were 99.999% pure discs (50mm diameter), placed 150 mm away from the substrate. The base pressure was less than 10^{-6} Torr, while sputtering was carried out in the presence of flowing argon, at a pressure of 2 mTorr. To ensure good homogeneity and crystallinity, a 450°C substrate temperature was used during deposition and the film thickness was monitored with a quartz oscillator during deposition. After deposition, the films were converted into VO_2 by controlled oxidization. Air was introduced to a pressure of 0.1Torr and the substrate temperature was held at 450°C for 5 hours.

X-ray diffraction patterns were obtained at room temperature showing the monoclinic phase of VO_2. High resolution scanning electron images showed columnar grains with diameters near 60 nm, as in the surface image in figure 1.

3.2 Optical characterisation

Optical measurements of spectral transmittance $T(\lambda)$ at normal incidence, and spectral reflectance $R(\lambda)$ at 8° off-normal incidence, were carried out using a Cary 5E UV-VIS-NIR spectrophotometer in the UV, visible and near-infrared over the wavelength range 2500 nm $\geq \lambda \geq$ 300nm. Sample heating was carried out with a home-made heater system designed for the spectrophotometer. The temperature was monitored by a thermocouple attached directly to the film surface. The spectra reported here were measured at 25°C and 80°C, which correspond to semiconductor and metallic phase of VO_2, respectively. A spectrum was also obtained at a temperature above 100°C to assess if plasmonic response was shifting with temperature rise. Optical hysteresis behaviour at the transition was studied by recording NIR transmittance at a wavelength of 2000 nm for every 1°C change in temperature. 2000 nm was chosen as a wavelength in the NIR which is representative of those where there is a large switching range in $T(\lambda)$ at the metal-insulator transition. Optical relative permittivity $\varepsilon(\omega)$ of metallic VO_2 at

frequency ω, and precise film thickness d, was obtained via a least squares simultaneous fitting of the complete set of T(λ) and R(λ) spectra with the Lorentz-Drude (LD) model of equation (1). ε(ω) is substituted in standard equations for T(λ) and R(λ) for thin VO_2 films of thickness d on a glass substrate. These equations use the well known Fresnel interface coefficients (r, t), plus the complex phase shift across the film $\delta(\omega) = \frac{2\pi}{\lambda}\varepsilon(\omega)^{1/2} d$. r and t define the complex field amplitude ratios of outgoing reflected or transmitted waves to those of the incoming waves at the air-film, film-glass and glass-air interfaces. (These relations are summarised in the Appendix).

$$\varepsilon(\omega) = \varepsilon_\infty + \sum_n \frac{A_n}{\omega_n^2 - \omega(\omega + i\omega_{\tau,n})} - \frac{\omega_p^2}{\omega(\omega + i\omega_\tau)} \qquad (1)$$

where ω_n are characteristic band-to-band transition energies, with $\omega_{\tau,n}$ the width of each transition and A_n their spectral weight. The Drude term, because of its significance to our analysis, is shown separately with ω_p the plasma frequency and ω_τ the conduction electron relaxation frequency. Only three oscillators plus the Drude term were required to achieve a best fit to our metal phase data over the experimental range of ω. If our films had a low energy transition near 0.7 eV, as found in some reported film data [4,10] a fourth oscillator would have been needed. Such an oscillator was tried but gave a worse fit, as was expected from the shape of our T(λ) and R(λ) plots around 1.5 μm. The term ε_∞ is included to account for the residual effect of higher frequency oscillators.

3.3 DC electrical properties

The DC electrical switching properties of VO_2 films were measured using the "ohms-per-square" method with a four-wire resistance measurement and evaporated electrodes. Data was acquired with 7552 Yokagawa digital multimeters, and automatically recorded using a LabView programme. Resistivity (ρ) can be calculated by multiplying the sheet resistance in ohms-per-square by the thickness of the film in centimetres and the conductivity $\sigma = 1/\rho$.

4. Results

4.1 Optical properties

Results for T(λ) and R(λ) in the semiconductor and metal phases (at 25°C and at 80 °C respectively), are presented in Figures 2 and 3 for 50 nm and 72 nm thick films of nano-grain VO_2 on glass. Both films display the large switching range expected in the NIR at these thicknesses.

The solid lines in figs.2 and 3 are curves of best fit using the model in equation (1) to the combination of data shown in figures 1 and 2 at each thickness. The resulting metal permittivity and Drude parameters for both films are tabulated in table 1 along with equivalent results from

Veleur et al [4] on 100 nm thick films on sapphire, and of Petit and Frigerio [10] on silica. Reference [4] data has been widely used in VO_2 theoretical modelling work, including modelling of nanoparticle absorption [2,5]. The main point of contrast is the complete absence in our data of a low energy transition (labelled NIR in table 1). Other parameters are in quite good agreement in the wavelength range relevant to optical switching and plasmonic response. The semiconductor phase spectral data was also fitted with equation (1), omitting the Drude term. Resulting Lorentz oscillator parameters are close for the two thicknesses, and also close to those reported in reference [4]. The metal phase transmittance fits in figure 2 are excellent at all wavelengths, but a systematic slight divergence from the simple Drude model curve is evident above 1.5 μm in the reflectance plots of figure 3 for the thinnest film,. This is less obvious but present for the 72 nm film. This small shift may be due to frequency dependence in key parameters.

Frequency dependent relaxation rates and plasma frequencies due to the d-electron correlations have been used previously to provide better fits to NIR data [9]. To further improve our longer wavelength fits we thus explored this possibility in a different and more self-consistent way, using a point-by-point $\varepsilon(\omega)$ fit [12] to yield the Drude model parameters at each wavelength above 1 μm. These parameters change smoothly with wavelength and yield an almost exact fit. The result for the 72nm film is, with frequency ω in units of eV,

$$\omega_p = 3.884 + 0.046\omega \text{ eV} \qquad (2)$$

but, as expected, relaxation rate does change more with ω. It cannot however fall to more "normal" metal values (< 0.1 eV say) by this ω dependence as seen in equation (3).

$$\omega_\tau = 0.745 + 0.13\omega(\omega - 1) \text{ eV} \qquad (3)$$

A weak ω^2 dependence for ω_τ is often found in metals due to electron-electron scattering [12] but we are not aware of any reports of an $\omega(\omega-1)$ behaviour. Frequency dependence here does not overcome the problem of the very high relaxation rate as claimed in reference 9, but they also needed a significant shift in effective mass and hence in ω_p to justify a low ω_τ value. Calculating the Drude parameters at each wavelength without any prior assumptions, rules out a significant shift in ω_P with frequency in our data.

A final optical result worth mentioning concerns the effect of a further elevation of temperature on Drude response. We find only a slight shift in NIR spectra at 120°C relative to those taken at 80° C. A slight change in relaxation rates would be enough to explain this but there is no evidence for a thermally activated shift in carrier density as might be expected from the unusual dc resistivity data and its associated small activation energy at the Fermi level, which we will discuss in the next section.

Table 1 Lorentz-Drude optical parameters for 50 nm and 72 nm thick films of VO_2 on glass with anomalous high temperature resistivity. Comparison to previously reported L-D permittivities includes data from reference [4] (as widely used data for theoretical modelling) and reference [10]. All ω values are in (eV) and A values in $(eV)^2$. Shaded rows are of prime importance in this study.

L-D oscillator parameter	**50 nm film VO_2 on glass**	**72 nm film VO_2 on glass**	**100 nm film on sapphire Ref.[4]**	**single crystal c-axis Ref. [4]**	**52 nm film on silica Ref.[10]**
ε_∞	4.45	5.09	3.95	4.17	1.74
ω_p	**3.22**	**3.90**	**3.33**	**4.2**	**2.78**
ω_τ	**0.72**	**0.71**	**0.66**	**1.25**	**1.21**
ω_{NIR}	**absent**	**absent**	**0.86**	**absent**	**0.26**
ω_1	2.79	2.78	2.8	2.94	2.72
ω_2	3.28	3.25	3.48	3.65	3.38
ω_3	3.94	3.84	4.6	5.3	5.12
$\omega_{\tau,NIR}$	**absent**	**absent**	**0.86**	**absent**	**0.37**
$\omega_{\tau,1}$	0.51	0.68	0.23	0.29	0.56
$\omega_{\tau,2}$	0.64	0.76	0.28	0.35	1.15
$\omega_{\tau,3}$	0.75	0.92	0.34	0.30	2.66
A_{NIR}	**absent**	**absent**	**1.34**	**absent**	**2.40**
A_2	3.72	5.56	7.62	7.17	2.91
A_3	6.9	9.69	12.6	16.0	8.33
A_4	10.5	12.1	22.2	50.6	39.5

4,2 Resistivity and hysteresis

Resistivity plots for heating and cooling through the transition appear in Figure 4 for a film close in thickness and of the same nanostructure to the 50 nm film in figures 1-3. Since we are contrasting optical switching with the shift in dc in electrical properties, we include a hysteresis plot of transmittance for this 50 nm film in Figure 5, at a wavelength of 2 μm. These hysteresis plots when compared, highlight the different switching temperatures between optical and resistance data. Switching in optical response on heating has a lower onset temperature than resistive switching by about 10°C and a higher onset temperature on cooling by about 4°C. NIR illumination may this facilitate the transition. Resistivity was recorded for T above T_c to near 150°C and the resulting log R versus 10^3/T plot is given in figure 6 for the metal phase data. Heating and cooling curves of this type exactly coincide and a linear straight line fit is also shown in figure 6. This line fits the data with a goodness of fit value of 0.9999. Resistivity is clearly continuing to fall as T rises to over 100° C above T_c and the associated thermal activation

energy $\Delta = 0.108 \pm 0.001$ eV. By comparison, the semiconductor state just below T_c in this film, has an activation energy for conduction of 0.16 eV, which is close to previously reported semiconductor activation energies of ~ 0.14 to 0.15 eV [13, 14] for T just below T_c. It is thus clear that the conduction mechanism occurring above T_c in these thin films involves different transitions. It is not simply a residual low T semiconduct..

Finally we compare the resistivity at 80° C estimated from our Drude parameters with the actual values at 80° C for the 50 nm film. Experimentally $\rho_{DC} = 4.5 \times 10^{-2}$ Ωcm while the Drude parameters on this film predict $\rho = 8.22 \times 10^{-5}$ Ωcm. By comparison large grain films 100 nm thick or more on sapphire [4, 6, 9] and single crystal samples [3] typically have ρ_{DC} around 2 to 3 x 10^{-4} Ωcm. Other reported nano-grain films [6] have similar ρ_{DC} to those in this study, from 3x 10^{-2} Ωcm to 3 x 10^{-3} Ωcm. The lower values occur at larger thicknesses and larger grain sizes. Our Drude results for the 72 nm film predict $\rho = 5.6 \times 10^{-5}$ Ωcm. Thus the lowest ρ_{DC} values reported are more than an order of magnitude above the values predicted from the Drude parameters in these strongest plasmonic systems. In our smallest grain size sample this difference is a factor of 550. Comparing to large grain samples, this film has a resistivity which is higher by a factor ~ 100. Given that these discrepancies cannot be attributed to any direct impact of additional defects in VO_2 on relaxation rates, which is the usual cause of higher resistivity, a more fundamental reason is indicated and is discussed in the next section.

5. Discussion

5.1 Optical Response

Using table 1 it can be deduced that these two nano-grain thin films have larger plasmonic response than bulk crystals or most other thin films for which comprehensive permittivity data has been reported. This superior response is due to the combination of one of the highest reported plasma frequencies, comparable relaxation rates to large grains, and the absence of an observable low energy transition. *These very small grains do not enhance the scattering rate, as might be expected in normal metals. This indicates that the unphysically high relaxation rate found in this and other studies is essentially intrinsic to metallic VO_2.* The observed relaxation rate is too high in the context of standard theories of electron transport in solids to be influenced directly by grain boundaries, even if they are just a few nm apart. Various explanations, usually related to specific sample features such as (unobserved) cracks, have been put forward to get around the problem of a high relaxation rate [3], but its presence in a diversity of structures indicates it is intrinsic. Our internally consistent approach to studying frequency dependence rather than forcing one parameter value to be constant, such as carrier density, indicates that some frequency dependence of relaxation rates due to the d-electron correlations is observable, but it is not enough to explain the high relaxation rates.

Other points of interest in the data are that electronic properties are changing with film thickness as well as grain size, as noted recently in other nano-grain studies [6]. Plasma

frequency is more sensitive to grain size and thickness than relaxation rate, again maybe because the latter is so high intrinsically. Either carrier density at the Fermi level or effective mass, or both, could be changing. Other experiments may be needed to resolve this issue and some are underway. An impact of thickness is an indication that one or both film surfaces may be having a significant influence, for instance by imposing additional stresses on neighbouring layers, which in turn shift electronic properties. As thickness increases the relative impact of surfaces should diminish. It is interesting that while the location of higher energy transitions, which are of secondary concern in this study, changes little, their width and hence spectral weight does change with thickness. Some impact of grain size on core as well as conduction electron properties in these nanograin systems is thus indicated. The observed grain sizes in SEM images such as fig.1 are near 60 nm, so they are too large to allow size dependent shifts in energy levels as found in some small semiconductor nanoparticles. However the frequency spread of these optical transitions might be sensitive to size, if for instance there was slight structural disorder. It is also possible the observed columns are not single grains.

5.2 Resistance-optical properties link

Our data, and that of others, shows that a stronger plasmonic NIR response does not translate into a higher dc conductivity and a narrower hysteresis curve. *The exact opposite is found.* Instead a thermally activated conductivity is found. However for a metal one expects not a rise, but a fall in conductivity with a linear T coefficient of resistive response, as found in single crystal data and expected in the presence of electron-phonon scattering [3]. Why is this happening in thin films with small grain size? For large crystals $\rho(T)$ switches at T_c by around 4 to 5 orders of magnitude and it then rises linearly with T. A sharp drop in ρ still occurs at T_c in our samples and in those of others with similar grain structure [6,8] but only by 2 to 2.5 orders of magnitude. As film thickness increases it appears this switching range also gradually rises. The resulting residual resistivity implies an incomplete transition. However the observed activation energy is not that in the semiconductor phase. Note also that the transmittance plot in Figure 5 is flat above T_c to 90°C as expected for the metal. It is interesting that the optical and resistive hysteresis curves in figures 4 and 5 have in common a change in slope in the cooling cycle curve at a round 50°C. This may be linked to the nanostructure or to the impact of the interface.

The origin of the apparent residual 0.l08 eV gap in small grain size samples and thin layers may provide new insights into VO_2 . Tunnelling barriers at miss-oriented grain boundaries might be possible but one would expect to see some activated response, even in larger grain systems. Thus some intrinsic effect enabled by either small grain size, or interface stresses, is more likely.

Since residual d-electron correlations can still influence VO_2 response in the metal state, they are a potential source of the high apparent intrinsic relaxation rate observed in both large and small grain systems, and in both optical and dc data. Can they also show up in other ways when there are many grain boundaries or local stresses, in particular in static fields? A high density of grain boundaries usually means a “dirtier” or more defective system for metallic electron transport, but in superconductors, which also involve strong correlations between electron pairs, plus quantum

coherence over a finite range, a “dirtier” electronic system can lead to type II behaviour and two transitions. The first transition is incomplete relative to its “pure” counterpart and the second is at much higher temperature. It is possible that our high density of defects (in the form of grain boundaries) play an analogous role by enabling some residual, but reduced strength pairing to persist to high temperatures. A related mechanism might involve quantum fluctuations due to transient pairing of transport electrons with those on neighbouring V sites. If these are the excited states or quasiparticles in this “metal” they may be able to fluctuate coherently in small grains, but become incoherent in large grains under dc fields, that is the coherence length could have a similar scale to our grain sizes. While normal Fermi liquid quasi-particle interactions or electron-electron scattering are usually relatively weak compared to electron-phonon scattering at our temperatures, these paired d-electron quasi-particles may scatter off each other strongly to yield the high intrinsic relaxation rates observed. High rates of interaction between quasi-particles are known to be conducive to coherence. Quantum coherence in solids at elevated temperatures is a topic of emerging current interest [15]. In this context, the differences and similarities between the optical and dc response in these nanostructures means that the excitations produced by NIR photons in a nanograin are not coherent while those arising in static fields are coherent. In both cases the excitations interact with each other or with unpaired excited electrons at a similar rate. Fluctuations might also lead to a kind of “metallic glass” or non-Fermi fluid electronic state, as postulated by Dobrosavljevic [16] and others [1]; with the transition to a normal Fermi fluid then requiring much higher temperatures.

These are complex issues for many-body transport and phase transition theory to resolve, and controlled and systematic experiments directed at further insights into these varied and structural dependent transport behaviours are needed to gain further insights. Quantum coherent effects at such high temperatures, while unexpected, are feasible [15]. Some VO_2 anomalies such as high relaxation rates are common to large grain and nano-grain systems, while the major differences between dc transport and optical data for these nanograin films seems to require a quantum based explanation. The resistive and optical property comparisons between nanoscale VO_2 samples and large grain size VO_2 are unusual and cannot be explained classically. A classical explanation based on increased carrier scattering does not apply, for two reasons : firstly because it is intrinsically too high to start with, and secondly because it would show up in both optical and dc data. For practical applications the focus will tend to be on optimizing for either dc or for optical switching, and this study indicates that for dc electrical work one will prefer quite different structures to applications needing optical switching.

6. Conclusion

Thin films of vanadium dioxide in the metallic phase, if they have very small grain sizes, can combine very strong plasmonic response and a complete optical switch to the metal phase at T_c, with an incomplete switch in dc response. When the dc switch is incomplete a thermally activated conductivity above T_c is found. Such behaviour with temperature is not found in large crystals or large grain size films. Quantum correlation effects could be behind this observation since

coherence among excitations is more likely in small grain structures, while scattering of such excitations off each other or off mobile electrons could explain the anomalous high relaxation rates at all grain sizes. High carrier relaxation rates have been found in this study and several others, and the overall evidence indicates they are intrinsic and not due to structure or defect based scattering.

We conclude on a practical note, by noting that nanoscale systems are to be preferred for optical switching applications, while dc electrical switching will work better with large grain systems.

Appendix

Thin film equations for the air-VO_2 film-glass system at normal incidence

Let the complex reflectance and transmittance Fresnel amplitude ratios at the air-film and film-glass interfaces be r_{af}, r_{fg}, t_{af}, t_{fg} . $\varepsilon(\omega)$ and film thickness d are the quantities to be modelled by least squares fitting to reflectance and transmittance data. They also determine the complex phase shift δ across the film, since $\delta = \frac{2\pi}{\lambda}\varepsilon^{1/2}d$.

At normal incidence

$$r_{af} = \frac{1-\varepsilon^{1/2}}{1+\varepsilon^{1/2}} \qquad \text{(a)}$$

$$r_{fg} = \frac{\varepsilon^{1/2}-\varepsilon_g^{1/2}}{\varepsilon^{1/2}+\varepsilon_g^{1/2}} \qquad \text{(b)}$$

$$t_{af} = \frac{2}{1+\varepsilon^{1/2}} \qquad \text{(c)}$$

$$t_{fg} = \frac{2\varepsilon^{1/2}}{\varepsilon^{1/2}+\varepsilon_g^{1/2}} \qquad \text{(d)}$$

These yield $R = r^*r + \Delta R_{sub}$ and $T = t^*t + \Delta T_{sub}$, with r , r* and t, t* complex conjugate pairs given by equations (e) and (f) and ΔR_{sub} and ΔT_{sub} small corrections due to the impact of the final glass-air interface. The latter are easily formulated exactly from the Fresnel coefficients in (a) to (d) plus r_{ga} and t_{ga}. They are included in the model assuming the film-glass and glass-air interfaces act incoherently on all rays crossing the thick glass substrate.

$$r = \frac{r_{af} + r_{fg} e^{i2\delta}}{1 + r_{af} r_{fg} e^{i2\delta}} \qquad \text{(e)}$$

$$t = \frac{t_{af} t_{fg} e^{i\delta}}{1 + r_{af} r_{fg} e^{i2\delta}} \qquad \text{(f)}$$

All r and t expressions are readily modified for arbitrary angles of incidence, but separate relations for rays which are polarised in the plane of incidence (p-waves) and normal to the plane of incidence (s-waves) must then be used.

Acknowledgements

We thank Ric Wuhrer for help with imaging, Geoff McCredie for assistance with coating work and Mike Cortie for encouraging us to work on VO_2.

References

1. Imada M, Fujimori A and Tokura Y 1998 Metal-insulator transitions *Reviews of Modern Physics* **70** 1039-1263
2. Lopez R, Feldman L C and Haglund R F 2005 Size dependent optical properties of VO_2 nanoparticle arrays *Phys. Rev. Lett.* **93** 177403
3. Allen P B, Wentzcovitch R M and Schultz W W 1993 Resistivity of the high-temperature metallic phase of VO_2 *Physixal Review B* **48** 4359-4363
4. Veleur H A, Barker A S and Berglund C N 1968 Optical Properties of VO_2 between 0.25 eV and 5 eV *Phys. Rev.* **172** 788-798
5. Suh J Y, Lopez R, Feldman L C, and Haglund R F Jr 2004 Semiconductor to metal phase transition in the nucleation and growth of nanoparticles and thin films *J. Appl. Phys.* **96** 1209-1213
6. Brassard D, Fournaux S, Jean-Jacques M, Kieffer J C and El Khakani M A 2006 Grain size effects on the semiconductor-metal phase transition characteristics of magnetron sputtered VO_2 thin films *Appl. Phys. Letts.* **87** 051910 1-4
7. Wang H, Yi X and Li Y 2005 Fabrication of VO_2 films with low transition temperature for optical switching applications *Optics Communications* **256** 305-309
8. Babulanam S M, Eriksson T S, Niklasson G A and Granqvist C G 1986 Thermochromic VO_2 films for energy-efficient windows *Proc. SPIE "Materials and Optics for Solar Energy Conversion and Advanced Lighting Technology"* **Vol. 692** 8-18
9. Choi H S, Ahn J S, Jung J H and Noh T W 1996 Mid-infra-red properties of a VO_2 film near the metal-insulator transition *Phys. Rev. B* **54** 4621 4628

10. Petit C and Frigerio J-M 1999 Optical properties of VO_2 thin films in heir dielectric and metallic states *Proc. SPIE "Europto Conference on Advances in Optical Inteference Coatings"* **Vol. 3738** 102-109
11. Biermann S, Poteryaev A, Lichtenstein A I and Georges A 2005 Dynamical singlets and correlation-assisted Peierls transition in VO_2 *Phys. Rev. Lett.* **94** 026404 1-4
12. Smith G B, Niklasson G A, Svensson J S E M and Granqvist C G 1986 Noble metal-based transparent infrared reflectors : experiments and theory for very thin gold films *J App. Phys.* **59** 571-581
13. Gavini A, and Kwan C Y 1972 Optical properties of semiconducting VO_2 films *Phys. Rev. B* **5** 3138-3143
14. Borisov B S, Koretskaya S T, Mokerov V G, Rakov A V and Solov'ev S G 1971 Electrical and optical properties of VO_2 near the semiconductor-semimetal transition point *Soviet Physics-Solid State* **12** 1763 -1769
15. Snoke D 2006 Coherent questions *Nature (News and Views)* **443** 403-404
16. Dobrosavljevic V, Tanaskovic D and Pastor A A 2003 Glassy behaviour of electrons near metal-insulator transitions *Phys. Rev. Lett.* **90** 016402 1-4

Figure captions

Figure 1 Scanning electron micrograph of the surface of a 50 nm thick VO_2 film on glass.

Figure 2 UV-Vis-NIR transmittance for 50 nm and 72 nm nanograin VO_2 films on glass. Continuous curves are best fits of the combined R and T data with a Lorentz-Drude oscillator model of equation (1).

Figure 3 UV-Vis-NIR reflectance for 50 nm and 72 nm nanograin VO_2 films on glass. Continuous curves are best fits of the combined R and T data with a Lorentz-Drude oscillator model of equation (1).

Figure 4 Resistance hysteresis across the transition with plot of metal phase resistance to 150°C for the 50 nm thick nanograin film . Cooling and heating curves overlap exactly for T > 80°C.

Figure 5 Hysteresis in transmittance at a wavelength of 2 μm .

Figure 6 Log of sheet resistance for the 50 nm thick VO_2 film as a function of inverse T($°K^{-1}$) for T above T_c.

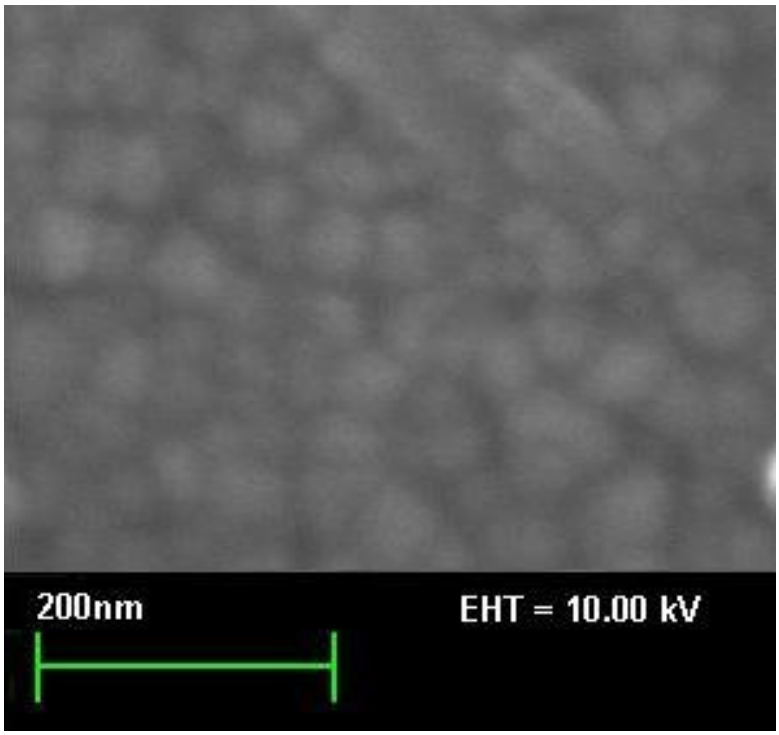

Figure 1

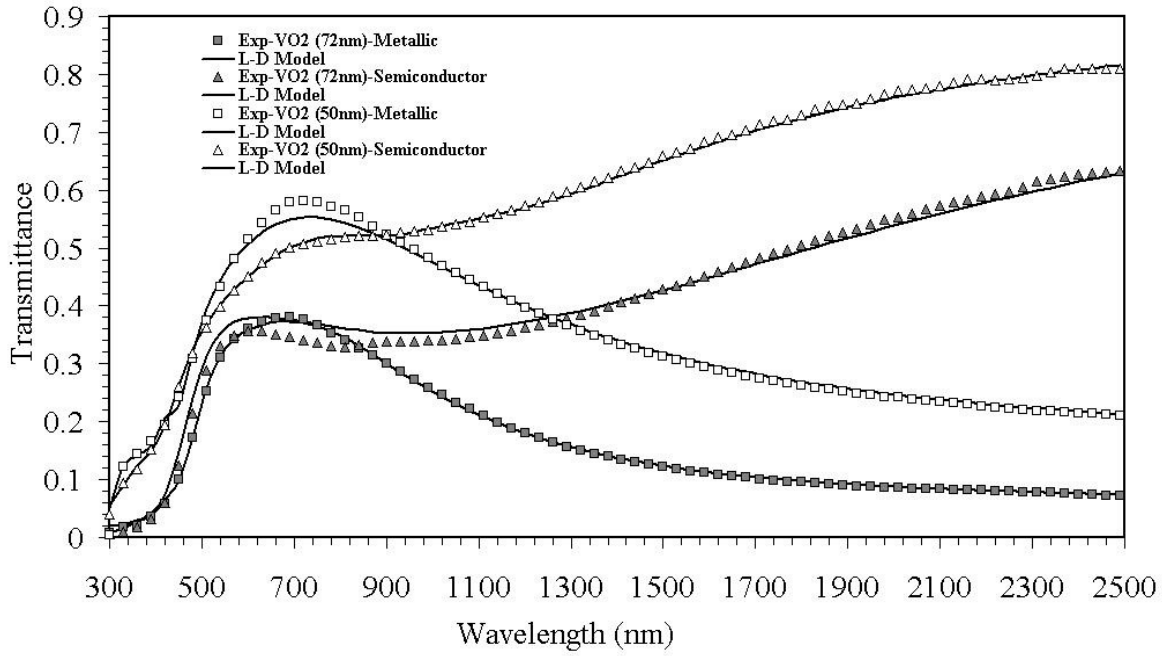
Exp-VO2 (72nm)-Metallic
L-D Model
Exp-VO2 (72nm)-Semiconductor
L-D Model
Exp-VO2 (50nm)-Metallic
L-D Model
Exp-VO2 (50nm)-Semiconductor
L-D Model
Transmittance
0.9
0.8
0.7
0.6
0.5
0.4
0.3
0.2
0.1
0
300
500
700
900
1100
1300
1500
1700
1900
2100
2300
2500
Wavelength (nm)

Figure 2

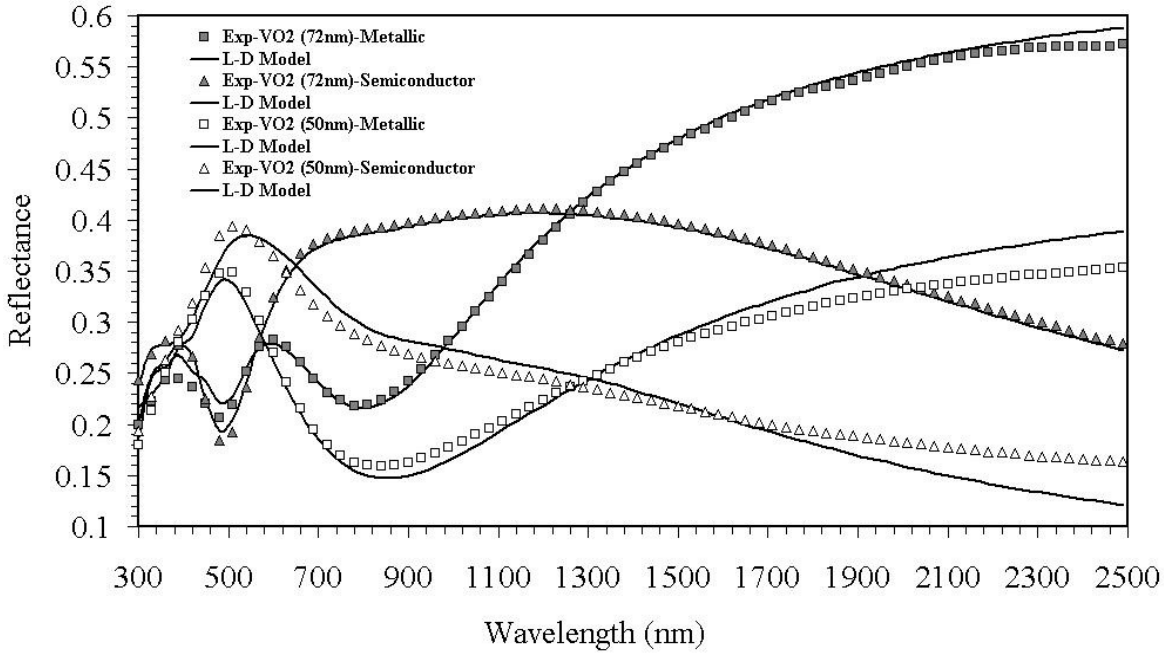
Exp-VO2 (72nm)-Metallic
L-D Model
Exp-VO2 (72nm)-Semiconductor
L-D Model
Exp-VO2 (50nm)-Metallic
L-D Model
Exp-VO2 (50nm)-Semiconductor
L-D Model
Reflectance
0.6
0.55
0.5
0.45
0.4
0.35
0.3
0.25
0.2
0.15
0.1
300
500
700
900
1100
1300
1500
1700
1900
2100
2300
2500
Wavelength (nm)

Figure 3

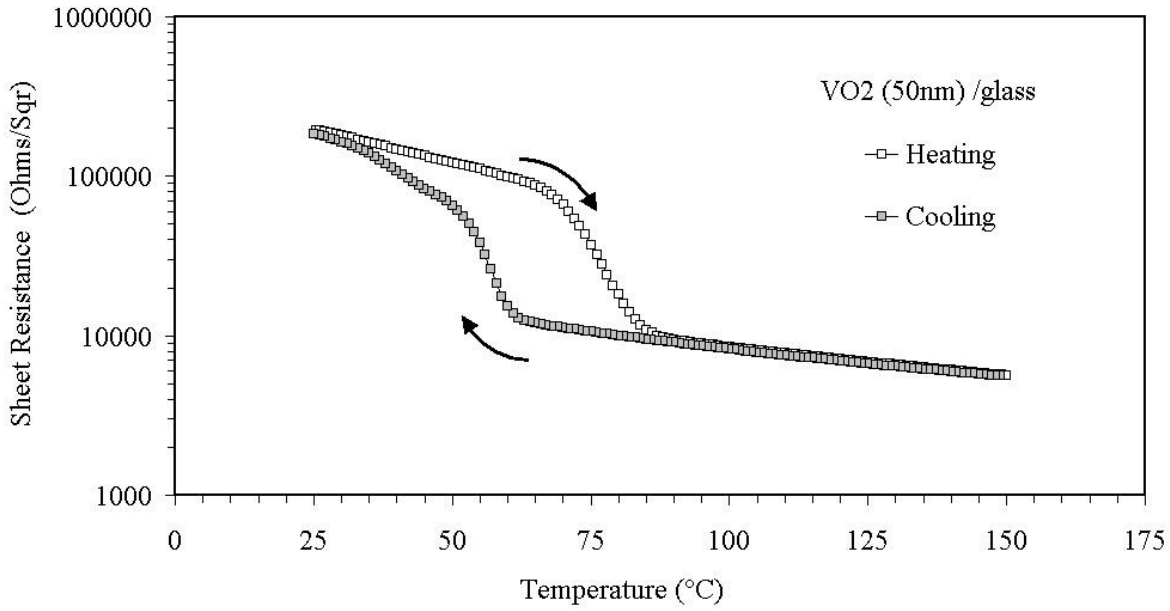
1000000
100000
10000
1000
Sheet Resistance (Ohms/Sqr)
0
25
50
75
100
125
150
175
Temperature (°C)
VO2 (50nm) /glass
Heating
Cooling

Figure 4

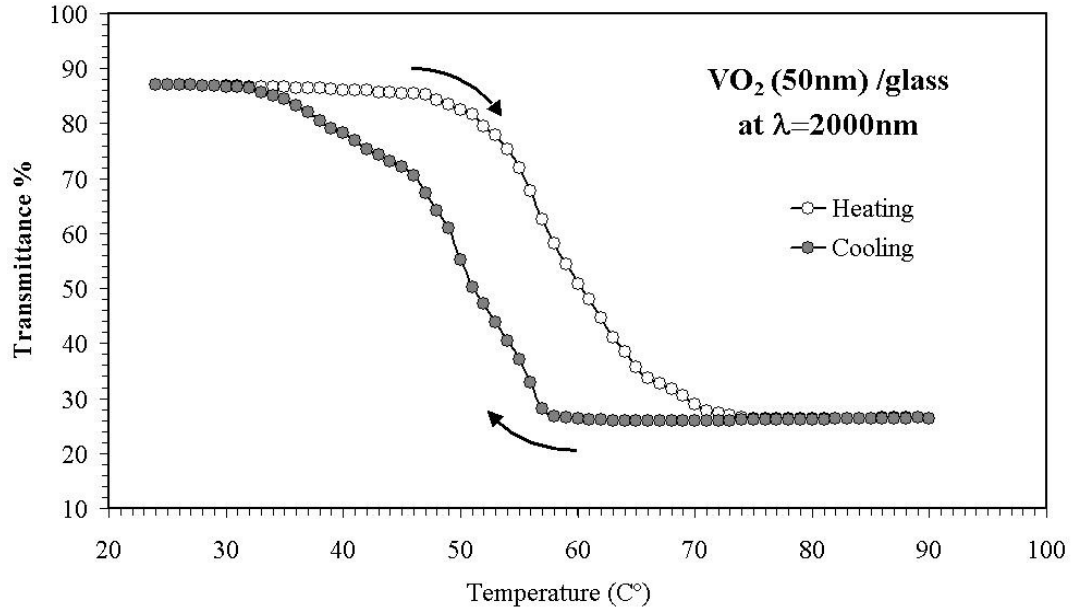
100
90
80
70
60
50
40
30
20
10
Transmittance %
20
30
40
50
60
70
80
90
100
Temperature (C°)
VO2 (50nm) /glass
at λ=2000nm
Heating
Cooling

Figure 5

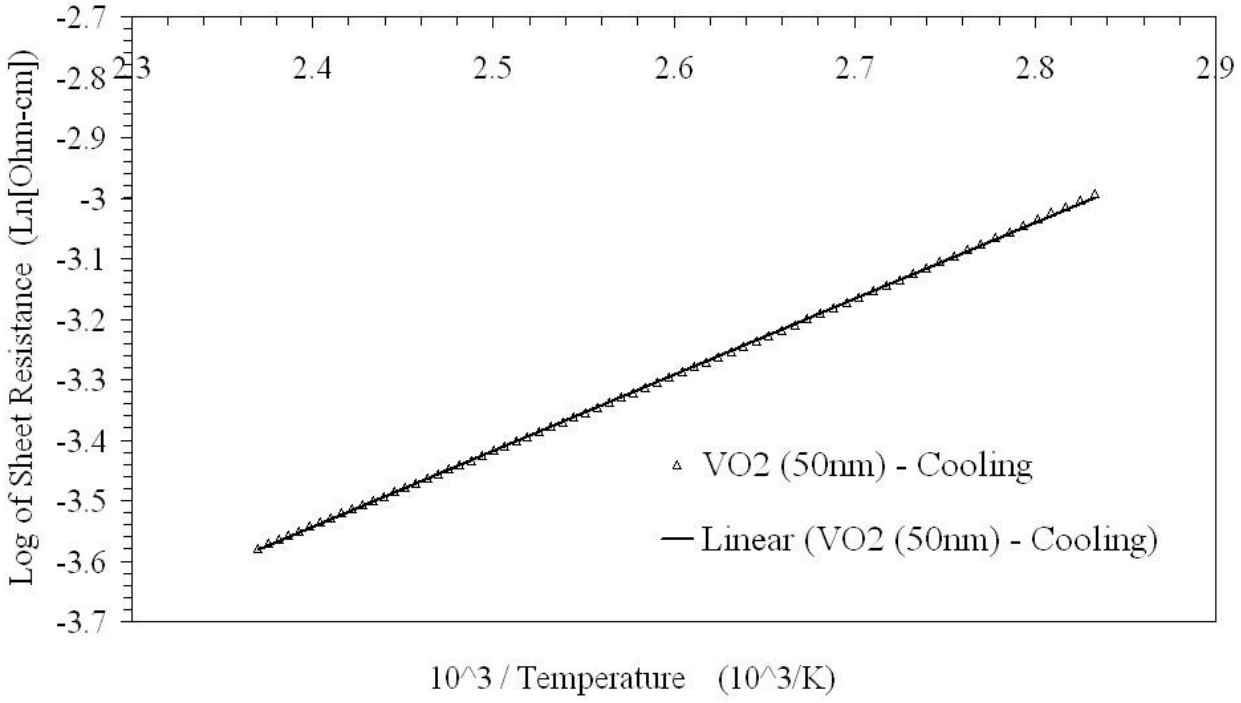
-2.7
-2.8
-2.9
-3
-3.1
-3.2
-3.3
-3.4
-3.5
-3.6
-3.7
2.3
2.4
2.5
2.6
2.7
2.8
2.9
Log of Sheet Resistance (Ln[Ohm-cm])
VO2 (50nm) - Cooling
Linear (VO2 (50nm) - Cooling)
10^3 / Temperature (10^3/K)

.

Figure 6